

A new triangular composite shell element with damping capability

This is a post-refereeing final draft. When citing, please refer to the published version:

K.Y. Sanliturk, H. Koruk, A new triangular composite shell element with damping capability, *Composite Structures* 118, 322–327, **2014**.
<https://doi.org/10.1016/j.compstruct.2014.07.053>

A new triangular composite shell element with damping capability

Kenan Y. Sanliturk^a, Hasan Koruk^{b,*}

^a*Istanbul Technical University, Mechanical Engineering Department, 34437 Istanbul, Turkey*

^b*MEF University, Mechanical Engineering Department, 34398 Istanbul, Turkey*

*Corresponding author, *Tel.:* +902122852814.

E-mail address: hasan.koruk@mef.edu.tr (H. Koruk)

Abstract

This paper presents a new triangular composite shell element with damping capability.

Formulation of the composite triangular shell element is based on stacking individual homogeneous triangular shell elements on top of each other. The homogeneous shell element is an assembly of a triangular membrane element with drilling degrees of freedoms and a plate element. Damping capability is provided by means of complex element stiffness matrix of individual flat layers of the composite element. These elements with damping capability allow modelling general structures with damping treatments. A few test cases are modelled using triangular finite element developed here and the results of the complex eigenvalue analyses are compared with those of the quadrilateral shell elements proposed recently. The results obtained using the presented triangular and previous quadrilateral composite elements are also compared with those based on modal strain energy method and experimental results. Comparisons of the experimental and the theoretical results confirm that the modal properties including modal damping levels of structures with damping treatments can be predicted with high accuracy using the proposed finite element.

Keywords: Triangular shell element; quadrilateral shell element; composite finite element; drilling degrees of freedom; complex eigenvalue problem.

1. Introduction

There are mainly three approaches for modelling damping in Finite Element (FE) applications

[1-6], namely; Direct Frequency Response, Modal Strain Energy (MSE) and Complex Eigenvalue methods. Direct Frequency Response method is very costly in terms of computation time as it requires computation of the frequency response function matrix at individual frequencies. Although, the MSE method can be used for modelling complicated damped structures, the assumptions associated with this method restrict its applicability for general use. In Complex Eigenvalue method, on the other hand, a complex eigenvalue problem needs to be solved without simplifying assumptions. Although Complex Eigenvalue method [7-9] is a known approach for the predictions of damping levels of structures, it has limited applications in practice.

Quadrilateral homogeneous and composite FEs based on complex eigenvalue method have been recently proposed by the authors of this paper [10]. However, the FE model (mesh) of a complex structure could not be generated using only quadrilateral elements, hence there is also a need for triangular elements. Therefore, a new composite triangular FE with damping capability is presented in this paper, the damping prediction being based on complex eigenvalue method again. The performances of the new composite triangular element and the quadrilateral one proposed before [10] are compared. The accuracy of the new composite triangular element is validated by comparing the theoretical predictions with experimentally determined natural frequencies and the associated damping levels using a few test structures. The FE formulation presented here allows modelling damped composite structures and performing modal analyses of the resulting complex eigenvalue problem so as to determine modal parameters including damping levels directly. The complex mode shapes of the structure are also obtained from the solution of the complex eigenvalue problem. The new triangular element together with the quadrilateral element developed before can be used to model complex composite structures in an effective way for damping prediction.

2. Composite triangular finite element with damping capability

Representing a multi-layered composite structure with an equivalent layer is an efficient way of modelling such structures as this approach does not yield excessive number of Degree of Freedoms

(DOFs) in the model [10]. However, the accuracy of the model depends on how each layer is represented and how the individual layers are assembled. The formulation of the composite triangular shell FE presented here is based on stacking individual homogeneous shell elements on top of each other as similar to the quadrilateral composite formulations presented by the authors of this paper before [10]. The shell FE in the current formulation also has an important feature in the sense that it has physical drilling DOFs θ_{zi} in the element normal (z) direction. This specific homogeneous shell element shown in Fig. 1 is a three-noded element which is the assembly of a triangular membrane element with drilling DOFs [11] and the plate element [12]. The formulations of the FEs proposed in [11-12] are implemented so as to obtain the element stiffness matrix \mathbf{k}_s . In this study, this basic triangular shell FE is also extended for dynamic analysis by computing the element mass matrix \mathbf{m}_s and also adding damping capability to the element by considering the complex Young's modulus of the material as $E^* = E(1 + j\eta)$ where E and η are the Young's modulus and the loss factor, respectively and $j = \sqrt{-1}$. The use of complex Young's modulus results in complex stiffness matrix \mathbf{k}_s^* for individual elements, a feature necessary to develop a composite element with damping capability.

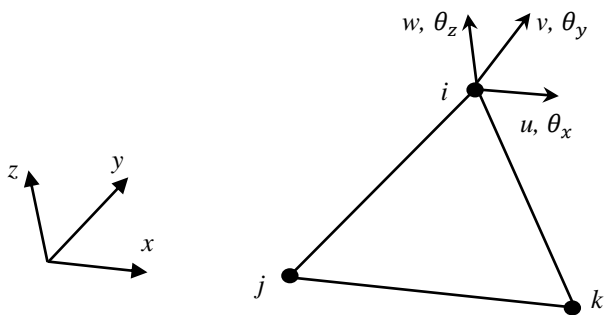


Fig. 1 Triangular flat shell element with six degrees of freedoms per node.

The connectivity definition and the element coordinate system for the composite element are shown in Fig. 2, the neutral plane being on the x-y plane. Beside the element coordinate system, the definition of the properties of the individual layers including the stacking order, layer thicknesses and the corresponding material properties are required in composite element formulation. One way of defining the stacking order and the corresponding thicknesses is to define the distance of the top surface of each layer from the bottom surface of the composite element, H_i , as illustrated in Fig. 3. So the individual thickness t_i as well as the distance of the mid-surface h_i for individual layers can be determined as

$$t_i = H_i - H_{i-1}; \quad h_i = 0.5(H_i + H_{i-1}) \quad i = 1, 2, \dots, n \quad (1)$$

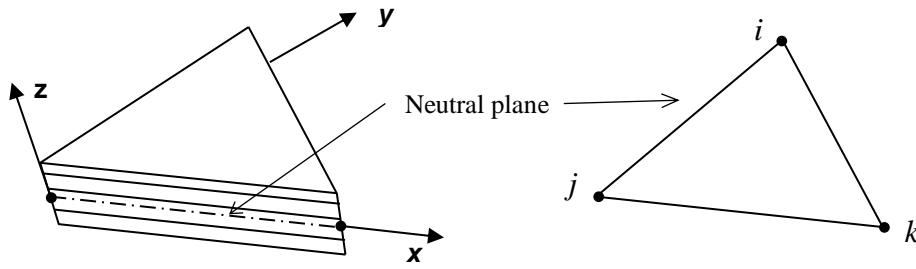


Fig. 2 Connectivity and geometry definition of the triangular composite element.

The individual layers of the composite element are assumed to be made of isotropic materials whose properties can be described by E_i , ν_i and η_i , representing the Young's modulus, Poisson's ratio and loss factor, respectively. The location of the neutral axis also needs to be determined for the formulation of the composite triangular element. Although it is not the case for the formulation of the homogeneous shell element, it is assumed here, only for the purpose of determination of the neutral axis, that the plane sections remain plane which allows the use of the basic bending formulation for the calculation of the distance of the neutral axis from the bottom surface of the composite element [10]. This leads to

$$h = \frac{1}{2} \frac{\sum_{i=1}^n E_i (H_i^2 - H_{i-1}^2)}{\sum_{i=1}^n E_i t_i} \quad (2)$$

The offset of the individual layers from the neutral axis can then be determined as $z_i = h_i - h$.

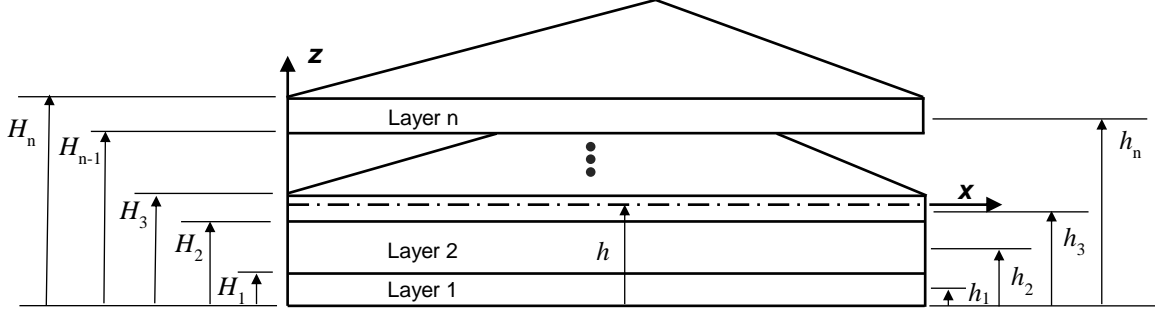


Fig. 3 Geometric definition of the triangular layers.

After the geometric parameters are determined, the composite triangular element can be formulated as follows. First, the stiffness and mass matrices for each layer (\mathbf{k}_{si}^* , \mathbf{m}_{si}) are computed as if each layer is oriented on the neutral plane. Then, the stiffness and mass matrices are transformed so as to take into account that each layer is actually offset from the neutral position by a distance z_i . This is performed by using the relationships between the nodal displacements and forces at the neutral plane and those at the offset location for individual layers. This can be expressed in matrix form as:

$$\mathbf{U}_i = \mathbf{T}\mathbf{U}_o \quad (3)$$

where

$$\mathbf{U}_i = [u_i \ v_i \ w_i \ \theta_{xi} \ \theta_{yi} \ \theta_{zi}]^T \quad (4)$$

$$\mathbf{U}_o = [u_o \ v_o \ w_o \ \theta_{xo} \ \theta_{yo} \ \theta_{zo}]^T \quad (5)$$

$$\mathbf{T} = \begin{bmatrix} 1 & 0 & 0 & 0 & z_i & 0 \\ 0 & 1 & 0 & -z_i & 0 & 0 \\ 0 & 0 & 1 & 0 & 0 & 0 \\ 0 & 0 & 0 & 1 & 0 & 0 \\ 0 & 0 & 0 & 0 & 1 & 0 \\ 0 & 0 & 0 & 0 & 0 & 1 \end{bmatrix} \quad (6)$$

The subscripts i and o above denote the locations of the layer i and the neutral plane, respectively and \mathbf{T} is the transformation matrix. It is worth stating that although the transformation matrix for elemental forces is slightly different than that shown in Eq. (6), it can be shown that the stiffness and mass matrices for individual layers can be expressed with respect to the neutral plane in a conventional manner as:

$$\mathbf{K}_{si}^* = \begin{bmatrix} \mathbf{T} & \mathbf{0} & \mathbf{0} \\ & \mathbf{T} & \mathbf{0} \\ & & \mathbf{T} \end{bmatrix}^T \mathbf{k}_{si}^* \begin{bmatrix} \mathbf{T} & \mathbf{0} & \mathbf{0} \\ & \mathbf{T} & \mathbf{0} \\ & & \mathbf{T} \end{bmatrix} \quad (7)$$

$$\mathbf{M}_{si} = \begin{bmatrix} \mathbf{T} & \mathbf{0} & \mathbf{0} \\ & \mathbf{T} & \mathbf{0} \\ & & \mathbf{T} \end{bmatrix}^T \mathbf{m}_{si} \begin{bmatrix} \mathbf{T} & \mathbf{0} & \mathbf{0} \\ & \mathbf{T} & \mathbf{0} \\ & & \mathbf{T} \end{bmatrix} \quad (8)$$

where $\mathbf{0}$ is a 6x6 zero matrix. Finally, the element stiffness and mass matrices for the composite element are obtained by adding the contributions of individual layers via a summation process as:

$$\mathbf{K}_c^* = \sum_{i=1}^n \mathbf{K}_{si}^* \quad (9)$$

$$\mathbf{M}_c = \sum_{i=1}^n \mathbf{M}_{si} \quad (10)$$

where the subscripts c above denotes the composite shell. Once the elemental stiffness and mass matrices are available with respect to the neutral plane, these matrices are transformed to a common global coordinate system and the natural frequencies and modal damping values for a damped system can be obtained by solving the standard eigenvalue problem:

$$(\mathbf{K}^* - \lambda^2 \mathbf{M}) \boldsymbol{\Psi} = \mathbf{0} \quad (11)$$

where \mathbf{K}^* and \mathbf{M} are the system stiffness and mass matrices, respectively. It is worth noting here that \mathbf{K}^* matrix is complex, representing non-proportional damping distribution. The complex eigensolution is obtained here by using Subspace Iteration Method [13] and the solution of the eigenvalue problem above yields complex eigenvalues λ_r^2 and eigenvectors (mode shapes) Ψ_r , respectively where r is the mode number. By defining $\lambda_r^2 = \omega_r^2 (1 + j\eta_r)$, natural frequencies and loss factors are given as $\omega_r^2 = \text{Re}(\lambda_r^2)$ and $\eta_r = \text{Im}(\lambda_r^2) / \text{Re}(\lambda_r^2)$. In what follows, the accuracy of the bare shell element is investigated first. Then, the performance of the composite shell element is demonstrated by comparing the predicted modal parameters of damped structures with measured values.

3. Validation of the homogeneous shell finite element

In this section, the performance of the homogeneous triangular shell element described above is evaluated. First, a cantilever steel beam with length $L = 220$ mm, width $w = 10$ mm and thickness $t = 1$ mm is modelled by using: i) the homogeneous triangular shell element developed here, ii) the quadrilateral shell element proposed before [10] and iii) the S4R shell element in Abaqus FE software [14]. The number of nodes used in individual models is kept constant (i.e.,135). The Young's modulus, loss factor, Poisson's ratio and density of the steel material are $E = 204$ GPa, $\eta = 0.001$, $\nu = 0.3$ and $\rho = 7866.7$ kg/m³, respectively. The results of theoretical modal analysis are then compared with experimental ones which are identified by analysing Frequency Response Functions (FRFs) measured using a non-contact excitation and response sensor. It is worth stating that the adverse effects of sensor attachments are eliminated here by the use of non-contact measurements, resulting in highly accurate experimental modal parameters [15-16]. Here, the non-contact exciter used in the test rig is capable of exciting the bending modes of the test structure, hence the predicted and the experimentally identified modal properties for bending modes are compared.

The predicted and experimentally identified natural frequencies for the first five bending modes of the cantilever beam are compared in Table 1. It is worth stating here that that the measured modal loss factors of the structure are identified to be about 0.12% for the given modes. As can be seen in Table 1, the predicted natural frequencies using the homogeneous triangular shell element presented in this paper and the quadrilateral shell element proposed before [10] are very close to the measured values, the natural frequencies predicted using the triangular element formulation being slightly higher (i.e., 0.09% times) than those predicted using the quadrilateral element. The average errors in predicted natural frequencies listed in Table 1 using the triangular shell, quadrilateral shell and the S4R shell elements in the model are $\epsilon = 0.32, 0.22$ and 0.58% , respectively. It is seen that both homogeneous triangular shell element presented in this study and the quadrilateral element presented before [10] perform better than the S4R shell element [14].

Table 1

Measured and predicted natural frequencies of a cantilever (steel) beam with $L = 220$ mm, $w = 10$ mm and $t = 1$ mm.

Bending Mode No., b	Experimental	Triangular Shell		Quadrilateral Shell [10]		S4R in Abaqus [14]	
	f_b (Hz)	f_b (Hz)	Error, ϵ_b (%)	f_b (Hz)	Error, ϵ_b (%)	f_b (Hz)	Error, ϵ_b (%)
1	16.99	17.06	0.42	17.04	0.32	17.04	0.28
2	107.02	106.93	-0.09	106.83	-0.18	106.89	-0.12
3	299.00	299.52	0.17	299.26	0.09	300.00	0.33
4	584.50	587.39	0.50	586.87	0.41	590.10	0.96
5	966.55	972.08	0.57	971.16	0.48	980.49	1.44

The performances of the new triangular shell element and the quadrilateral shell element [10] are evaluated using the bending modes of a cantilever beam above. However, the investigation of the performance of the shell elements here is not limited to bending modes only; the vibration modes of a plate structure are also examined. The dimensions of the plate are selected so that the plate would have no symmetrical modes and the modes would also not be closely spaced for accurate experimental modal identification. The dimensions of the plate are: $L = 300$, $w = 200$ and $t = 1$ mm. The Young's modulus, loss factor, Poisson's ratio and density of the plate material are $E = 206$ GPa, $\eta = 0.001$, $\nu = 0.3$ and $\rho = 7665$ kg/m³, respectively. Preliminary measurements of frequency

response functions on the plate showed that the accelerometer provided additional damping.

Therefore, non-contact measurements are preferred; modal parameters of the plates are determined using the spectrums of acoustic pressure signals acquired via a microphone in the acoustic free field [17-18].

The plate is again modelled using three different shell elements, namely, the homogeneous triangular shell element, quadrilateral shell element presented before [10] and the S4R shell element in Abaqus [14]. The individual shell models have 2501 nodes. The measured and predicted natural frequencies of the plate with free-free boundary conditions are listed in Table 2 where p and q represent the number of half-waves in a mode shape along the long and short edges, respectively. The experimental modal loss factors of the plate for the given modes are about $\eta_r = 0.1\%$. It is seen that the predicted and measured natural frequencies match very well as the average errors between the theoretical and the experimental natural frequencies are 0.67%, 0.64% and 0.82% for the triangular, quadrilateral and the S4R shell in Abaqus, respectively. The results show that the performances of both quadrilateral and triangular shell elements are excellent and slightly better than the performance of the S4R element. In the next section, the performance of the triangular composite element with damping capability is evaluated.

Table 2

Measured and predicted natural frequencies of a plate with $L = 300$ mm, $w = 200$ mm and $t = 1$ mm.

Mode		Experimental	Triangular Shell		Quadrilateral Shell [10]		S4R in Abaqus [14]	
No., r	(p,q)	f_r (Hz)	f_r (Hz)	Error, ϵ_r (%)	f_r (Hz)	Error, ϵ_r (%)	f_r (Hz)	Error, ϵ_r (%)
1	(2,2)	57.1	57.3	0.36	57.3	0.33	57.4	0.47
2	(3,1)	61.1	61.2	0.08	61.2	0.08	61.2	0.11
3	(3,2)	132.4	132.2	-0.11	132.2	-0.16	132.4	0.00
4	(1,3)	141.8	142.6	0.60	142.6	0.61	142.7	0.69
5	(4,1)	164.4	164.8	0.28	164.8	0.26	165.0	0.40
6	(2,3)	188.3	191.4	1.68	191.4	1.66	191.7	1.82
7	(4,2)	244.5	245.0	0.22	244.9	0.16	245.4	0.37
8	(3,3)	280.1	282.0	0.68	281.7	0.59	282.4	0.82
9	(5,1)	341.1	343.0	0.54	343.0	0.55	344.1	0.86
10	(1,4)	377.2	386.0	2.33	385.9	2.32	387.1	2.64

4. Evaluation of the composite finite element with damping capability

A few test cases are used for evaluation and validation of the new triangular composite element with damping capability. The predicted modal parameters are compared with those of the quadrilateral composite element [10], the MSE method [10, 19] and experimental results. Four different damping materials, labelled as materials A, B, C and D, are used to treat the individual base structures, the material properties of the damping materials being listed in Table 3. The material of the base structures is steel, the mechanical properties being given in the previous section. The Poisson's ratio is taken as 0.45 for damping materials.

Table 3
Young's moduli and loss factors of the damping materials.

Material	ρ (kg/m ³)	f (Hz)	E (MPa)	η (%)
A	2372.0	98	1050	32.8
		275	1070	42.6
		538	1070	50.6
B	2312.9	104	1520	28.8
		308	2060	24.6
		618	2320	23.3
C	2312.9	90	447	42.6
		253	469	50.3
D	2218.8	92	554	46.2
		261	616	47.4

Here, using the aforementioned material properties, a few structures including a fully-damped cantilever beam, a partially-damped cantilever beam and a damped U-plate are modelled using (i) the new triangular composite shell element presented in this paper; (ii) the quadrilateral composite shell element [10] and (iii) the FE approach based on the MSE method. The S4R shell element in Abaqus [14] is used to calculate strain energies of individual layers of a composite structure required for damping estimations based on MSE method. Mesh convergence check is made and an appropriate mesh size is used; 5 mm mesh size for the triangular and quadrilateral shell elements and 2.5 mm mesh size for the S4R shell element in Abaqus.

It is known that the material properties of viscoelastic damping materials depend on frequency. Therefore, it is not possible to make appropriate predictions of more than one natural frequency of

the composite structures using a single eigenvalue (modal) analysis. Therefore, it is necessary to specify the material properties for a specific frequency range and then perform the modal analysis applicable to that frequency range only. The frequency range and the corresponding material properties are changed accordingly and the modal analysis of the damped structure is repeated until the whole frequency range of interest are analysed.

First, a fully-damped cantilever beam is studied. The fully-damped beam is made by coating a layer of damping material A to one side of the base beam. The dimensions (length and width) of this beam are $L = 220$ mm and $w = 10$ mm, respectively. Thickness of the base (steel) beam is $t = 1$ mm while the thickness of the damping layer is $t_1 = 2.2$ mm. Three different FE models are developed for the same damped beam. FE models with composite elements are created using 4x44 triangular and 2x44 quadrilateral composite finite elements. The third FE model is created using 4x88 S4R elements in Abaqus for each layer. It is worth restating here that the modal properties of only the bending modes of cantilever beam are measured using the test rig utilising non-contact excitation and response sensors. Therefore, comparisons are made only for the bending modes of the damped cantilever beam. Experimentally determined and predicted natural frequencies and loss factors using the composite triangular element, the quadrilateral element [10] and the MSE method for the damped cantilever beam are listed in Table 4. It is seen that the predicted loss factors and natural frequencies via new composite triangular element are very close to the experimentally identified values as well as to the predictions made by using the quadrilateral composite shell element [10] and those of the MSE method. These results clearly confirm the performance and the validity of the new composite FE formulation presented in this study.

Table 4

Experimental and predicted natural frequencies of a fully-damped cantilever beam with $L = 220$ mm, $w = 10$ mm and $t = 1$ mm.

Bending Mode No., b	f_b (Hz)	η_b (%)	f_b (Hz)	η_b (%)	f_b (Hz)	η_b (%)	f_b (Hz)	η_b (%)
	Experimental		Triangular		Quadrilateral [10]		MSE	
2	97.93	9.219	98.38	9.443	98.27	9.415	98.28	9.430
3	274.64	12.129	276.18	12.364	275.90	12.341	275.96	12.390
4	537.67	14.513	541.17	14.637	540.65	14.611	540.98	14.700

A partially-damped cantilever beam whose modal properties are also identified experimentally is also modelled and the results are evaluated. The total length of the partially-damped beam is $L = 250$ mm and the length of the coated damping layer (using damping material B) is $L_1 = 220$ mm (i.e., the length of the bare part between the fixed end of the beam and the damping layer is 30 mm). The width of the beam is $w = 10$ mm, and the thickness of the base and the damping layer are $t = 1$ mm and $t_1 = 2.2$ mm, respectively. The damped regions of the partially-damped cantilever beam are modelled using the composite finite elements while the other regions are modelled by using the homogeneous shell elements. The measured and the predicted results of this partially-damped cantilever beam are listed in Table 5. As seen, the predicted results are very close to the measured ones again, demonstrating once again that the new triangular composite FE formulation presented in this paper yield high accuracy.

Table 5

Experimental and predicted natural frequencies of a partially-damped cantilever beam with $L = 250$ mm, $L_1 = 220$ mm, $w = 10$ mm, $t = 1$ mm and $t_1 = 2.2$ mm.

Bending Mode No., b	f_b (Hz)	η_b (%)	f_b (Hz)	η_b (%)	f_b (Hz)	η_b (%)	f_b (Hz)	η_b (%)
	Experimental		Triangular		Quadrilateral [10]		MSE	
2	78.28	7.890	76.65	7.928	76.59	7.924	76.56	7.944
3	233.80	9.110	231.32	9.137	231.16	9.136	231.15	9.158
4	471.73	9.468	471.23	9.455	470.90	9.456	471.06	9.492

Relatively a more complex structure, U-plate, is also studied here. The U-plate is made of steel and partially treated using two different damping materials (C and D). The individual thicknesses of these two damping materials are the same, $t_1 = 2.2$ mm. FRF measurements are performed on the damped U-plate in free-free conditions using a modal hammer and an accelerometer. The FE model of the plate obtained using triangular shell elements including the dimensions and damping patches are illustrated in Fig. 4. As in the partially-damped cantilever beam, damped regions of the U-plate are modelled using the composite shell FEs and the other regions are modelled using homogeneous shell elements. The damped U-plate is also modelled using the FE approach based on the MSE method.

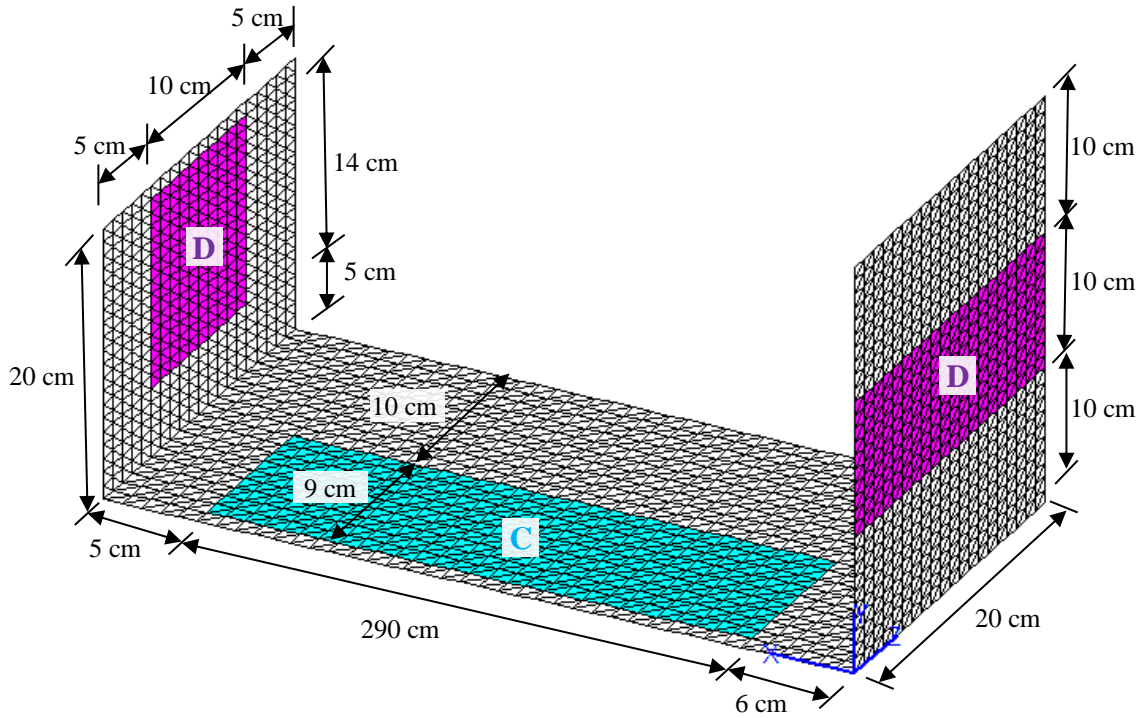


Fig. 4 U-plate structure with three damping patches and corresponding dimensions.

The predicted and experimentally identified natural frequencies and modal loss factors of the damped U-plate are listed in Table 6 and presented graphically in Fig. 5. Results show that the natural frequencies predicted by using the new triangular composite element and the quadrilateral composite shell element in [10] and the MSE method are very close to the experimental natural frequencies. It is seen, both qualitatively and quantitatively, that the predicted loss factors are very close to the experimentally identified values, confirming that the composite triangular element presented in this paper as well as the previous quadrilateral composite element are capable of predicting the damping levels for individual modes with high accuracy. It should be stated here that, although the MSE method can be used for modelling damped structures, the assumptions associated with this method restrict its applicability for general use. However, the formulations of new triangular elements together with the previous quadrilateral elements based on Complex Eigenvalue method allow the complex eigenvalue problem being solved without simplifying assumptions and can be used for general applications.

Table 6

Experimental and predicted natural frequencies of a U-plate structure treated with a few damping materials.

Mode No., r	f_r (Hz) η_r (%)		f_r (Hz) η_r (%)		f_r (Hz) η_r (%)		f_r (Hz) η_r (%)	
	Experimental		Triangular		Quadrilateral [10]		MSE	
1	14.62	0.491	13.62	0.500	14.59	0.487	14.66	0.486
2	28.89	0.522	26.35	0.491	29.13	0.484	29.31	0.483
3	33.98	0.423	33.96	0.488	33.94	0.441	34.13	0.441
4	70.07	0.603	71.83	0.599	72.29	0.600	72.63	0.603
5	73.56	0.476	77.91	0.531	73.35	0.523	73.78	0.524
6	106.76	0.455	114.16	0.498	108.87	0.514	110.03	0.517
7	120.41	0.913	122.29	0.855	121.75	0.866	122.20	0.872
8	130.20	0.445	134.27	0.475	131.97	0.476	132.49	0.474
9	188.93	0.712	195.85	0.627	188.70	0.708	190.04	0.708
10	223.16	0.571	234.38	0.620	232.75	0.612	234.04	0.615
11	272.38	0.744	285.12	0.557	272.60	0.719	274.16	0.723
12	277.35	0.494	290.31	0.577	281.98	0.516	283.62	0.514
13	333.99	0.755	346.97	0.666	343.98	0.649	344.47	0.658
14	360.44	0.727	371.90	0.714	367.33	0.747	368.26	0.743
15	375.71	0.987	395.96	0.865	389.63	1.007	390.22	1.010

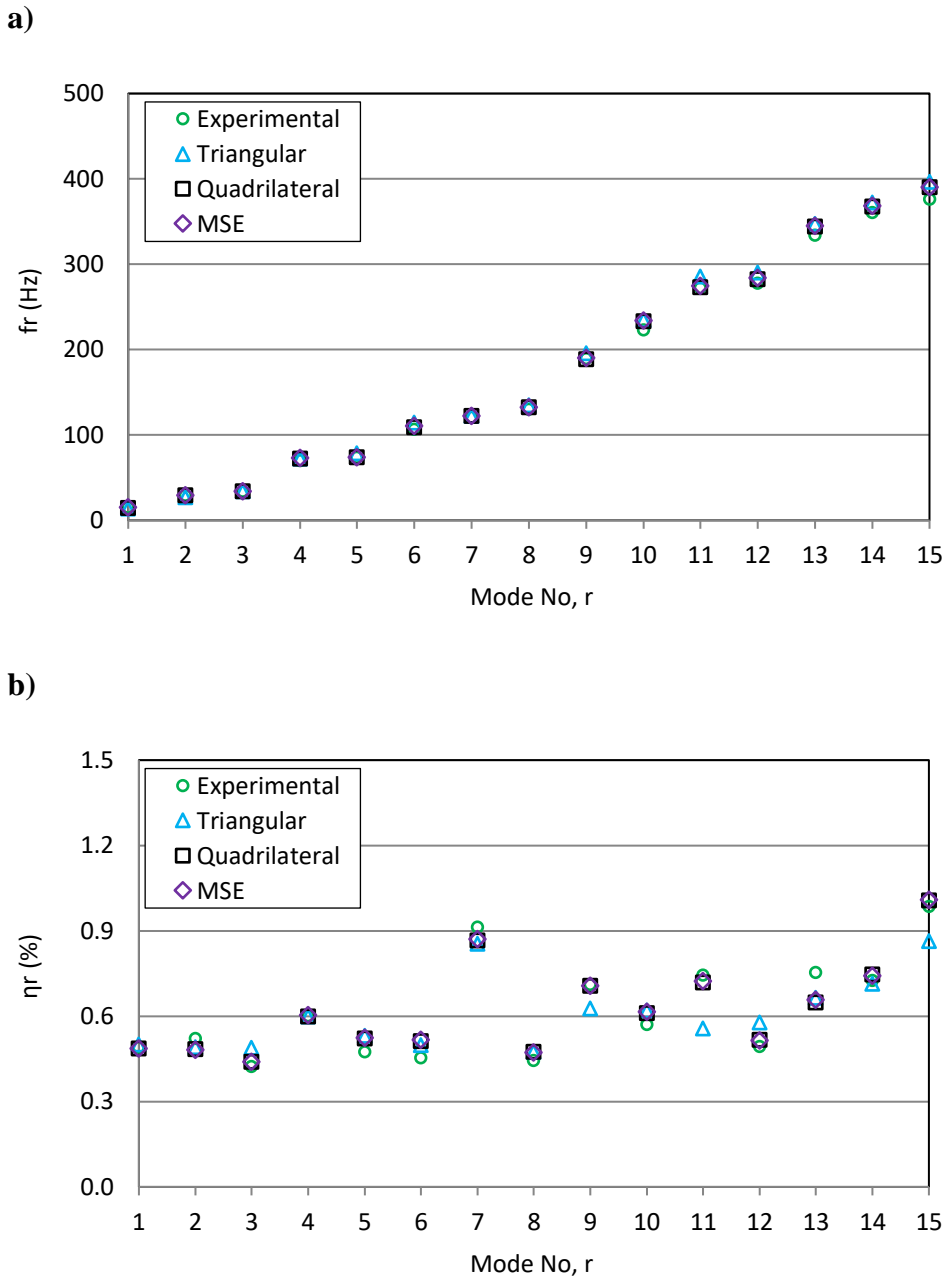


Fig. 5 Experimental and predicted natural frequencies (a) and loss factors (b) of a U-plate structure identified using triangular and quadrilateral shell elements and the MSE method.

5. Conclusions

In this study, the formulation of a new composite triangular shell finite element with damping capability is presented. The formulation of the triangular composite element is based on stacking individual three-noded shell elements, that have physical drilling degrees of freedom for the rotation in the direction perpendicular to the element surface, on top of each other. The individual

homogeneous layers of the composite elements can have different material properties and the damping capability is included in the formulation by means of complex elemental stiffness matrix. Following the formulation and implementation of the composite element based on Complex Eigenvalue method, the performance of the homogeneous triangular shell FE is evaluated. Then, the composite element is validated by comparing the theoretical predictions with experimentally determined natural frequencies and the associated damping levels using a few test structures.

The performances of both the new triangular and previous quadrilateral homogenous shell elements are excellent. Comparisons of the measured and the predicted results indicate that the new triangular composite shell element and previous quadrilateral composite shell element yield high level of accuracy in predicting modal parameters of damped structures. It should be stated that, in contrast to the MSE method, the formulation based on complex eigenvalue method allows the complex eigenvalue problem being solved without simplifying assumptions and can be used for general applications. The new triangular elements together with quadrilateral ones can be used to model any complex structure in an effective way.

References

- [1] Johnson CD, Kienholtz DA. Finite element prediction of damping in structures with constrained viscoelastic layers. *AIAA J* 1982;20:1284-90.
- [2] Rao MD, Echempati R, Nadella S. Dynamic analysis and damping of composite structures embedded with viscoelastic layers. *Compos Part B* 1997;28:547-54.
- [3] Gounaris GD, Anifantis NK. Structural damping determination by finite element approach. *Comput Struct* 1999;73:445-52.
- [4] Plagianakos TS, Saravanos DA. Mechanics and finite elements for the damped dynamic characteristics of curvilinear laminates and composite shell structures. *J Sound Vib* 2003;263:399-414.

- [5] Rastogi N. Forced frequency response analysis of multimaterial systems. In: Proceedings of SAE Noise and Vibration Conference and Exhibition, Grand Traverse, MI, USA, 2005.
- [6] Zhang SH, Chen HL. A study on the damping characteristics of laminated composites with integral viscoelastic layers. *Compos Struct* 2006;74:63-69.
- [7] Bathe K-J. *Finite Element Procedures in Engineering Analysis*. Prentice-Hall; 1982.
- [8] Bathe K-J. *Finite Element Procedures*. Prentice-Hall; 1996.
- [9] Cortés F, Elejabarrieta MJ. An approximate numerical method for the complex eigenproblem in systems characterised by a structural damping matrix. *J Sound Vib* 2006;296:166-82.
- [10] Sanliturk KY, Koruk H. Development and validation of a composite finite element with damping capability. *Comput Struct* 2013;97:136-46.
- [11] Ibrahimbegovic A, Frey F. Membrane quadrilateral finite elements with rotational degrees of freedom. *Eng Fract Mech* 1992;43:13-24.
- [12] Ibrahimbegovic A. Quadrilateral finite elements for analysis of thick and thin plates. *Comput Method Appl M* 1993;110:195-209.
- [13] FINES: Finite Element for Structures. Istanbul Technical University, Mechanical Engineering Department, Istanbul, 2012.
- [14] Abaqus 6.9.1. Finite Element Software, 2010.
- [15] PULSE LabShop 17.1.0, Sound and Vibration Measurement Software, Bruel and Kjaer, Copenhagen, Denmark, 2013.
- [16] ICATS: Imperial College Testing Analysis and Software, Imperial College, Dynamic Section, London, 2010.
- [17] Koruk H, Dreyer JT, Singh R. Modal analysis of thin cylindrical shells with cardboard liners and estimation of loss factors. *Mech Syst Signal Pr* 2014;45:346-349.
- [18] Koruk H. Quantification and minimization of sensor effects on modal parameters of lightweight structures. *J Vibroeng* 2014;16(4):1952–63.

[19] Koruk H, Sanliturk KY. Optimisation of damping treatments based on big bang - big crunch and modal strain energy methods. *J Sound Vib* 2014;333(5):1319-30.